

## Paleomagnetic Constraints on Ages of Mineralization in the Kalahari Manganese Field, South Africa

D. A. D. Evans,

*Tectonics Special Research Centre, University of Western Australia, Crawley, WA 6009, Australia*

J. GUTZMER, N. J. BEUKES,

*Department of Geology, Rand Afrikaans University, Auckland Park 2006, Johannesburg, South Africa*

AND J. L. KIRSCHVINK

*Division of Geological and Planetary Sciences, 170-25, California Institute of Technology, Pasadena, California 91125*

### Abstract

We report paleomagnetic data from samples spanning several grades of enrichment in the Kalahari manganese field, South Africa, in order to assess mineralogical aspects of the ore-forming stages, and also to date these stages through comparison to previously existing, well dated paleomagnetic results from the Kaapvaal-Kalahari craton. Our paleomagnetic study confirms a multistage evolution for the orebodies, with three distinct, ancient remanent directions preserved. An early diagenetic remanence direction (MAM-1), associated with "dusty" hematite inclusions (1-10,um) that are omnipresent in the microcrystalline matrix of low-grade, Mamatwan-type ore, yields a tilt-corrected paleomagnetic pole ( $08.2^\circ$  N,  $111.1^\circ$  E,  $dp = 5.6^\circ$ ,  $dm = 11.1^\circ$ ;  $n = 6$  specimens) that is similar to previous results from the immediately underlying Ongeluk lavas. A late diagenetic or weak metamorphic overprint (MAM-2), carried by recrystallized hematite (20-250 um), within both Mamatwan- and Wessels-type ore, generates a paleomagnetic pole (present coordinates  $12.1^\circ$  N,  $321.8^\circ$  E,  $dp = 3.4^\circ$ ,  $dm = 6.0^\circ$ ; tilt-corrected  $16.1^\circ$  N,  $317.8^\circ$  E,  $dp = 3.4^\circ$ ,  $dm = 6.4^\circ$ ;  $n = 14$  specimens) that resembles those from the ca. 1900 Ma Hartley lavas and Mashonaland sills. The MAM-2 overprint may be related to Kheis thrusting at 1750 to 1800 Ma as previously proposed or to magma-driven fluid migration during rifting as the Hartley-Mashonaland igneous event perforated the Kalahari craton. The third magnetic component observed in our sample suite (WESS) is restricted to high-grade Wessels-type ore, rich in high Fe hausmannite and coarser hematite (0.1-1.0 mm), in the immediate vicinity of north-trending normal faults. It yields a pole ( $54.4^\circ$  N,  $033.7^\circ$  E,  $dp = 4.7^\circ$ ,  $dm = 9.1^\circ$ ;  $n = 7$  specimens) that is similar to both the ca. 1250 and 1100 Ma portions of the Kalahari craton's apparent polar wander path. Either of these ages would be in accordance with previous multigenetic models for the Wessels event and its regional crosscutting relationships. Our WESS paleomagnetic pole, combined with previous paleomagnetic results from the Sishen-Postmasburg region, temporally links Kalahari manganese field hydrothermal upgrading with east vergent thrusting in the Griqualand West foreland, during the early or medial stages of the late Mesoproterozoic Namaqua orogeny

### Introduction

THE MANGANESE ores of the giant Kalahari manganese field (Cairncross et al., 1997) occur as three laterally continuous, stratiform beds that define the centers of symmetrical Superior-type iron- and manganese formation chemical sedimentary cycles (Beukes, 1983), deposited shortly after a Paleoproterozoic glaciation of perhaps global extent (Evans et al., 1997; Tsikos and Moore, 1998; Kirschvink et al., 2000). Together the iron- and manganese-rich cycles constitute the Early Paleoproterozoic Hotazel Formation, with an age of ca. 2200 Ma (Cornell et al., 1996) or 2400 Ma (Bau et al., 1999). The Hotazel Formation lies conformably between the underlying Ongeluk lavas and the overlying dolomitic Mooirdraai Formation. The strata are very gently folded, dipping westward  $5^\circ$  to  $15^\circ$  throughout the Kalahari manganese field. Two main ore types are present in the Kalahari manganese deposit (Cairncross et al., 1997): low-grade carbonate-rich Mamatwan-type ore (30 and 39 wt % Mn) and high-grade oxide-rich Wessels-type ore ( $>42$  wt % Mn).

Low-grade Mamatwan-type ore (Kleyenstüber, 1984; Nel et al., 1986) constitutes 97 percent of the total ore reserves and may be described as a microcrystalline (grain sizes below 10 um), finely laminated mudstone composed of kutnahorite ( $\text{CaMn}(\text{CO}_3)_2$ ), first-generation braunite ( $\text{Mn}_7\text{SiO}_{12}$ ), and hematite (I; roman numerals in parentheses denote order of generation). Abundant millimeter-sized ovoids of kutnahorite, recrystallized hematite (Ib), and braunite occur in this microcrystalline matrix, which is thought to be of sedimentary or early diagenetic origin (Kleyenstüber, 1984). This Mamatwan-type ore represents the proto-ore to a series of subsequent metamorphic, hydrothermal, and supergene alteration events (Gutzmer and Beukes, 1996); all but two of these alteration events are only of very localized importance, with alteration restricted to the immediate vicinity of joints, veins, or erosional unconformities. The first regional alteration involves late diagenetic or metamorphic replacement of kutnahorite by a first generation of hausmannite ( $\text{Mn}_3\text{O}_4$ ), accompanied by some recrystallized hematite (II), Fe-poor bixbyite ( $(\text{Mn,Fe})_2\text{O}_3$ ), and Mn calcite. Such replacement is concentrated along specific strata in the Mamatwan-type ore as bedding-parallel veinlets or replacement products of carbonate

<sup>1</sup> Corresponding author: emad, devans@src.uwa.edu.au

laminae or ovoids (Nel et al., 1986). Hausmannite (I) occurs as coarse, subhedral to euhedral crystals containing less than 3 wt percent  $\text{Fe}_2\text{O}_3$ . Gutzmer and Beukes (1996) tentatively linked this fluid flow to thrusting and crustal thickening from the west during the Kheis orogenic event at ca. 1700 to 1800 Ma (Stowe, 1983; Cornell et al., 1998).

The second (Wessels) event of structurally controlled hydrothermal alteration is restricted to the northern part of the Kalahari deposit, an area affected by east-verging thrust duplication and north-northeast-trending normal faulting (Fig. 1). Virtually all high-grade ore in the Kalahari manganese field (about 3% of the total ore reserve) formed when low-grade Mamatwan-type ore was metasomatically transformed to oxidized and coarsely crystalline Wessels-type ore (cf. Beukes et al., 1995; Gutzmer and Beukes, 1995). Fluid inclusion studies

(Lüders et al., 1999) and mass-balance calculations (Gutzmer and Beukes, 1997) have illustrated that upgrading of manganese ore from Mamatwan to Wessels type occurred within a low-temperature (<250°C) hydrothermal metasomatic system by residual enrichment of Mn at the expense of Mg, Ca,  $\text{CO}_2$ , and  $\text{SiO}_2$ . It has previously been uncertain if hematite (I) and late diagenetic and/or metamorphic hausmannite (I) were consumed during this alteration, because both minerals occur widely in both altered and unaltered ores. Available geochronological constraints, although merely quoted without any accompanying analytical data, suggest that the Wessels alteration event took place at ca. 1300 Ma (Dixon, 1989).

A preexisting system of Paleoproterozoic north-south-trending normal faults (Beukes and Smit, 1987) acted as feeder channels for hydrothermal fluids during the Wessels alteration event (Gutzmer and Beukes, 1995). A distinct zonation of mineral assemblages is developed around these feeder faults, reflecting an increase in degree of metasomatic alteration with increasing proximity to the faults (Fig. 1B). Gutzmer et al. (1995) established the presence of two distinct types of hausmannite (II) in these high-grade Wessels-type ores. Type (IIa) is generally finer grained (0.1-0.5 mm diam) and contains between 3 and 12 wt percent  $\text{Fe}_2\text{O}_3$ . This Fe-rich hausmannite is succeeded by much coarser crystalline, Fe-poor hausmannite (IIb) that contains less than 5 wt percent  $\text{Fe}_2\text{O}_3$  and has grain sizes ranging between 0.5 and 3 mm. Block samples of ore containing Fe-rich hausmannite (Ma) were found to be strongly magnetic, with unblocking temperatures between 400° and 500°C (Gutzmer et al., 1995).

The manganese ore bed is intensively hematitized and silicified immediately adjacent to the normal faults (Gutzmer and Beukes, 1995). These ferruginized zones are physically distinct from the high-grade hausmannite ores. Petrographic examinations reveal several events of hematite formation and recrystallization (III, IV, etc.) recorded within the ferruginized and silicified fault areas, suggesting multiple events of fluid flow and possible reactivation of the faults.

We collected paleomagnetic samples from the main Mn-bearing bed of the Hotazel Formation, altered to various degrees (Fig. 1B): unaltered Mamatwan-type ore, Wessels-enriched hausmannite ore, and hematitic ore adjacent to fault zones of the Wessels event. In addition, we sampled footwall jaspilite iron-formation with a high degree of Wessels alteration. The sample suite was selected in order to identify, by comparing and contrasting remanent magnetic directions, aspects of mineralogical association among the various ore-forming episodes. In addition, we sought to compare our resulting paleomagnetic poles to those previously determined (and well dated) from the Kalahari craton, in order to date the various mineralization styles in a manner independent of existing isotopic constraints (Dixon, 1989). Our results could serve not only to refine the model described above but also to test between that model and the fundamentally different hypotheses of single-stage Mn enrichment throughout the Kalahari manganese field during deposition of the Hotazel Formation (Cornell and Schitte, 1995; see also Beukes and Gutzmer, 1996) or during Mesoproterozoic hydrothermal alteration (de Villiers, 1983, 1992).

The paleomagnetically relevant minerals occurring among our sample suite are the different generations of hematite and

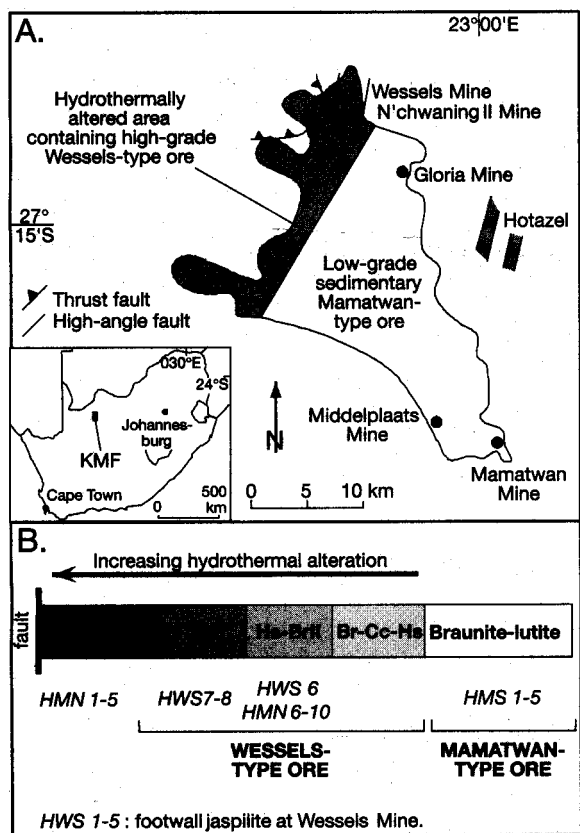


FIG. 1. Geologic framework of paleomagnetic samples collected from the Kalahari manganese field (KMF), after Beukes et al. (1995). A. Location map for sampled mines in the KMF. B. Location of samples within the previously recognized Mamatwan-Wessels alteration sequence. Braunite-lutite = least altered Mamatwan-type ore, dominated by braunite (I), kutnahorite, and very fine grained hematite. Br-Cc-Hs = coarse-grained hausmannite (II), associated with some manganese and calcite proto-ore, replaces kutnahorite; braunite (I), hausmannite (I), and hematite (I) apparently remain unaffected at this low degree of alteration (not sampled). Hs-BrII = increasing metasomatic alteration forms braunite II (an Si-depleted braunite, not a second generation of braunite s.s.) and coarse crystalline hausmannite (II); these two minerals are associated with minor specularite, variable amounts of other manganese oxides (e.g., bixbyite, manganite, marokite), and minor amounts of numerous other mineral phases (e.g., sparitic calcite, gaufreyite, barite, andradite, clinocllore, etc.; Gutzmer and Beukes, 1996). Hs = almost pure hausmannite; the highest grade ore formed during the Wessels alteration event. Br = second-generation braunite (II) forming a narrow zone marginal to the hematitized fault zone (not sampled).

possibly the high Fe hausmannite (Table 1). Although Gutzmer et al. (1995) implicated strong magnetization of the Wessels-type hausmannite (II) orebody to properties of the high Fe hausmannite alone, further experiments (Baron et al., 1998) found that model untenable. Subsequent analyses have likewise eliminated Mn-rich hematite as a possible cause for the strong magnetization of Wessels-type ore (J. Gutzmer and V Baron, unpub. data) and thus the strong ferromagnetic properties of Wessels-altered hausmannite (II) ore are yet unexplained. Jacobsite ( $\text{Fe}_2\text{MnO}_4$ ; Curie temperature ca. 290°C) is widespread throughout some strata within the Kalahari manganese field (Gutzmer and Beukes, 1996) but is undetectable within our samples from the braunite-lutite orebodies and their Wessels-altered correlatives. The bixbyite solid solution ( $(\text{Mn}, \text{Fe})_2\text{O}_3$ ) is paramagnetic at temperatures above ca. 80 K (Grant et al., 1968), as is braunite (Abs Wurmbach et al., 1981; Taneja and Garg, 1993); these phases thus cannot contribute to magnetic remanence in the Kalahari manganese field.

### Methods

We sampled from three working mines in the Kalahari manganese field: Mamatwan, N'chwaning II, and Wessels. The first area has not been upgraded to Wessels-type ore, whereas the latter two are immediately adjacent within the Wesselsenriched zone (Fig. 1). Samples were either drilled as 2.5-cm-diam oriented cores in the field or collected as oriented blocks and drilled in the laboratory. Right-cylinder specimens of 2.2-cm length were cut from the cores and measured on a 2G-Enterprises cryogenic (SQUID) magnetometer in the Caltech paleomagnetic laboratory. Thermal and static alternating-field demagnetization steps sequentially reduced each specimen's natural remanent magnetization (NRM) into its constituent components, which were found to have nonoverlapping demagnetization spectra. Thermal demagnetization was aborted when either the magnetic intensity attained the

noise level of the magnetometer or when spurious, strongly magnetized components appeared (despite field maintenance of <10 nT throughout the furnace system). Field and demagnetization techniques varied among the sampled sites and are discussed below on an individual basis. All directional data were regressed via least-squares fitting of linear segments within the demagnetization trajectories (Kirschvink, 1980). The small number of samples collected in this reconnaissance-type study preclude calculation of truly reliable paleomagnetic poles for the purposes of continental reconstruction (cf. Van der Voo, 1990), yet in all but one instance (noted below) our observed data are unambiguous and define clear directional groupings whose means should not differ substantially through further analyses.

#### Mamatwan (samples HMS 1-5)

Five oriented block samples were collected from three different levels of the open-pit mine (Nel et al., 1986). One block was cut into two cores, generating a total of six analyzed specimens. Dips of bedding at the sampling sites varied between 7° and 14° to the west-northwest. Following measurement of NRM, alternating-field demagnetization steps were 10, 15, and 20 mT; then thermal steps of 150°, 220°, 250°, 280°, 300°, 325°, 355°, 400°, 450°, 500°, 525°, 545°, 555°, 565°, 600°, 625°, and 665°C. Some specimens were further heated to 675° and 700°C. From the doubly cored block, a second specimen was subjected first to alternating-field demagnetization steps at intervals of 5 mT to a maximum of 80 mT, followed by the aforementioned thermal schedule.

#### N'chwaning II (samples HMN 1-10)

Ten oriented blocks were sampled from the underground mine, Section 48 South. The blocks' azimuthal orientations were determined by triangulation from the mine survey grid. Five samples (HMN 1-5) are from a hematitized zone within a secondary, high-angle fault that cuts the entire succession,

TABLE 1. Ferromagnetic Properties of Remanence-Bearing Phases in the Kalahari Manganese Field

Phase <sup>1</sup>	Paragenesis	Ore stage <sup>2</sup>	Grain size	Unblocking temperature (°C)		Samples	Directional component
				Expected <sup>3</sup>	Observed		
Hematite(I) ( $\text{Fe}_2\text{O}_3$ )	Early diagenetic	Braunite-lutite	1-10 $\mu\text{m}$	-675	675-700	HMS 1-5	MAM-1 (W horizontal)
Hematite(II)	Late diagenetic- early metasomatic	Br-Cc-Hs, Hs-BrII, Hs	20-250 $\mu\text{m}$	<<675	200-400	HMS 1-5, HMN 6-10, HWS 6-8	MAM-2 (WNW down)
High Fe Haus- mannite (IIa) ( $\text{Mn}_3\text{O}_4$ )	Late metasomatic	Br-Cc-Hs, Hs-BrII, Hs	0.1-0.5 mm	400-500	325-500	HMN 6-10, HWS 6-8	WESS (S subhoriz.)
Hematite(III)	Late metasomatic	Hs-BrII, Hs	0.1-1.0 mm				
Hematite (IV) ±maghemite	Latest metasomatism of Wessels event	Fault zone	1 $\mu\text{m}$ - >>1 mm	Broad Range	400-540, 675-700	HWS 2-5, HMN 2-5	WESS (high scatter)

<sup>1</sup> Parenthetic roman numerals indicate generation sequence of multiply formed phases

<sup>2</sup> See Figure 1

<sup>3</sup> Sources: Pullaiah et al. (1975), Gutzmer et al. (1995); see text

and the other five (HMN 6-10) are from high-grade Wessels-type Mn ore in a hydrothermally altered zone adjacent to the fault (Fig. 1). Bedding dips 12° toward 246°. One sample from each group (HMN 1, 8) was not analyzed but retained for petrographic study. Samples HMN 2-5 were measured at NRM, followed by demagnetization steps of 5 to 20 mT, and further at 150°, 250°, 350°, 450°, 540°, 580°, 600°, 610°, 625°, 640°, 655°, 665°, 675°, and 700°C. From the high-grade, Wessels-type Mn ore adjacent to the fault zone (HMN 6-10), five specimens were cored from the four blocks. Following measurement of NRM, specimens were subjected to alternating-field demagnetization at 20 mT, then thermal demagnetization at 150°, 220°, 250°, 280°, 300°, 325°, 350°, 400°, 450°, and 500°C.

#### Wessels (samples HWS 1-8)

We sampled eight blocks in the Hotazel Formation, ascending in upward stratigraphic sequence, along the conveyor shaft serving as access to the mine crusher. All sample orientations were triangulated relative to the shaft's north-south axis as gridded on the mine plan. Bedding at Wessels dips 5° toward 285°. Samples HWS 1-5 are from the basal jaspilite iron-formation immediately overlying the Ongeluk lavas; samples HWS 6-8 lie within bedded Mn formation. Although no fault zone is observed precisely at this locality, all samples have been subjected to Wessels-type alteration that is clearly fault related throughout the nonwestern sector of the Kalahari manganese field (Beukes et al., 1995). Sample HWS-1 was retained for petrographic analysis. The other jaspilites (HWS 2-5) were measured at the same steps as HMN 2-5 (see above). The Mn-rich samples (HWS 6-8) were measured in the same sequence as HMN 6-10 but with an extra thermal step of 525°C; further demagnetization was

not attempted because magnetic intensity had dropped to near zero (less than 0.1% of NRM) by the final step.

#### Paleomagnetic Results

Our combined dataset comprises three well clustered magnetic components (Tables 1, 2). From Mamatwan, two are observed: a west-northwest downward component removed completely by 400°C or primarily by 35 mT, and a stable endpoint, west horizontal component removed entirely between 675° and 700°C and stable above 80 mT (Fig. 2). This latter component (MAM-1) is most likely carried by hematite (I), which is omnipresent as microcrystalline diagenetic inclusions in the braunite- and kutnahorite-rich low-grade ore at the Mamatwan mine (Gutzmer and Beukes, 1996). The ~1- to 10  $\mu$ m grain size for these hematite inclusions implies that they are single domain (cf Dunlop and Ozdemir, 1997), a conclusion consistent with them carrying the extremely stable MAM-1 remanence. The west-northwest downward component (MAM2), with unblocking temperatures between 100° and 400°C, is probably carried by neoformed hematite (II), ubiquitously present in the Mamatwan-type orebodies (Gutzmer and Beukes, 1996). The coarser grain size (20-250  $\mu$ m) of this second hematite generation places it within the transitional state between single and multidomain behavior (Kletetschka et al., 2000). Dominance of NRM by the soft, MAM-2 component is also consistent with the coarser grain size of hematite (II). Rock magnetic results from the HMS samples (Fig. 3A) confirm these conclusions, showing coexistence of a high coercivity phase, most certainly hematite (I), with another remanence carrier of moderate median coercivity, probably hematite (II).

Manganese-rich samples from N'chwaning II (HMN 6-10) and Wessels (HWS 6-8) revealed a west-northwest downward component with similar direction and unblocking-temperature

TABLE 2. Paleomagnetic Results from the Kalahari Manganese Field<sup>1</sup>

Component (samples) <sup>2</sup>	n/N	T <sub>unbl</sub> (°C)	Present coordinates				Tilt-corrected coordinates				
			D (°)	I (°)	k	$\alpha_{95}$ (°)	D (°)	I (°)	k	$\alpha_{95}$ (°)	
<b>MAM-1</b>											
HMS 1-5	6/6	675-700	276.6	-00.4	29.8	12.5	<u>276.4</u>	<u>-10.8</u>	<u>38.2</u>	<u>11.0</u>	
Paleomagnetic pole: (-08.2°N, 111.1°E, dp = 5.6°, dm = 11.1°)											
<b>MAM-2</b>											
HMS 1-5	6/6	200-400	301.8	33.6	68.0	8.2	300.7	23.3	46.7	9.9	
HMN 6-10	5/5	220-325	296.2	34.5	106.7	7.4	300.2	25.0	103.8	7.5	
HWS 6-8	3/3	220-325	280.1	35.0	202.8	8.7	280.3	30.1	198.7	8.8	
Combined	14/14		<u>295.2</u>	<u>34.5</u>	<u>59.2</u>	<u>5.2</u>	<u>296.4</u>	<u>25.6</u>	<u>45.8</u>	<u>5.9</u>	
Paleomagnetic pole—present coordinates: (12.1° N, 321.8° E, dp = 3.4°, dm = 6.0°)											
Paleomagnetic pole—tilt-corrected coordinates: (16.1° N, 317.8° E, dp = 3.4°, dm = 6.4°)											
<b>WESS</b>											
HMN 6-10	4/5	325-500	186.1	-12.6	62.7	11.7	185.3	-01.9	65.2	11.5	
HWS 6-8	3/3	325-500	186.5	-19.9	32.4	22.0	184.8	-18.8	31.4	22.4	
Combined	7/8		<u>186.3</u>	<u>-15.7</u>	<u>48.5</u>	<u>8.8</u>	185.1	-09.1	32.8	10.7	
HWS 2-5 <sup>3</sup>	4/4	400-540	156.0	-32.9	22.9	19.6	153.6	-29.4	22.1	20.0	
Paleomagnetic pole: (54.4° N, 033.7° E, dp = 4.7°, dm = 9.1°)											

<sup>1</sup> Abbreviations: n/N = number of specimens included in mean/number analyzed; T<sub>unbl</sub> = unblocking temperature spectrum; D, I = mean declination, inclination; k = Fisher's (1953) precision parameter;  $\alpha_{95}$  = radius of 95 percent confidence cone about mean; underlined = directions used to calculate paleomagnetic poles

<sup>2</sup> Site locations: HMS (27.4° S, 023.0° E); HMN, HWS (27.1° S, 022.9° E); reference locality used for computing MAM-2 paleomagnetic pole: (27.2° S, 022.9° E)

<sup>3</sup> Not used in final calculation of paleomagnetic pole

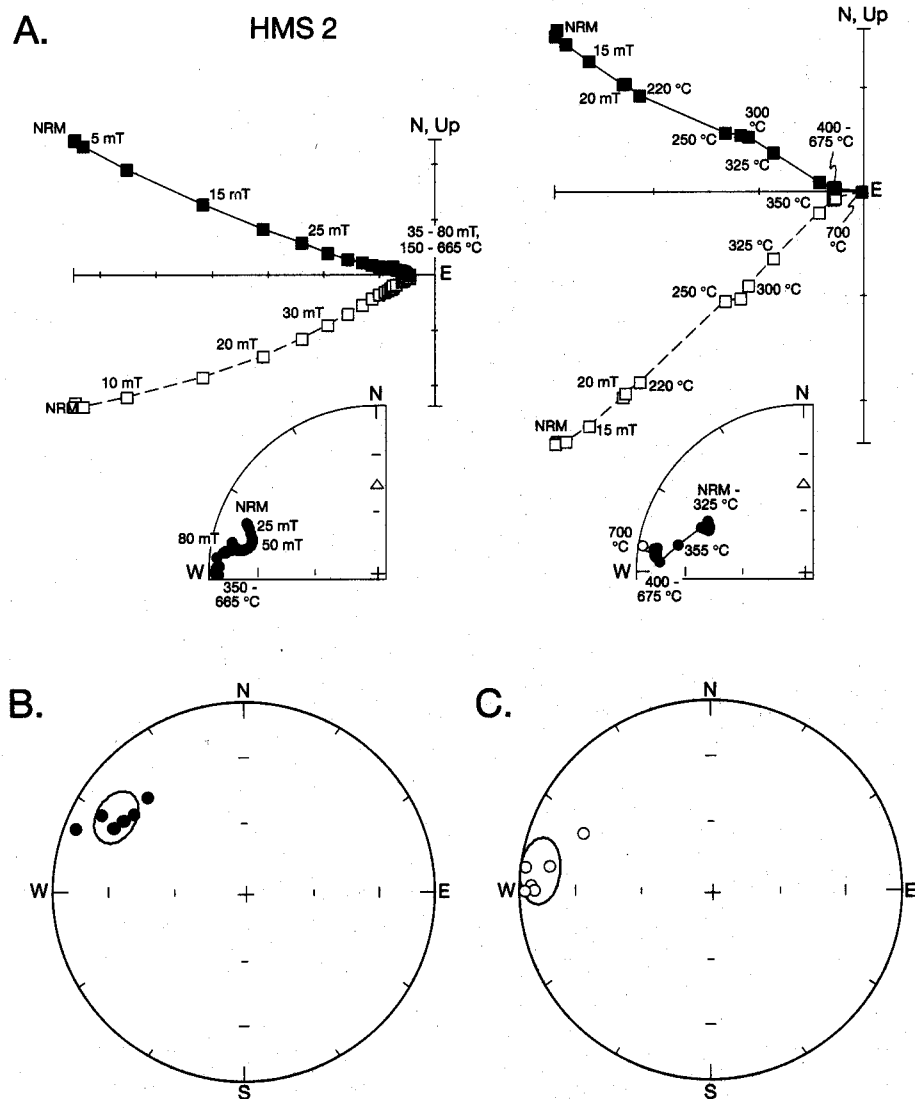


FIG. 2. Paleomagnetic data from Mamatwan (HMS). A. Representative demagnetization behavior in specimens HMS 2.1 and HMS 2.2, in present (in situ) coordinates. B. Least-squares MAM-2 component directions and their Fisher (1953) mean, depicted by 95 percent confidence oval. C. Tilt-corrected least-squares MAM-1 component directions and their Fisher distribution mean. Superimposed orthogonal projection plots: solid = horizontal plane, open, dashed = north-south and vertical plane, tick marks 10, <sup>-2</sup> A/m. Equal-area plots: solid = lower hemisphere, open = upper hemisphere; triangle = present dipole field direction at sampling locality. NRM = natural remanent magnetization.

spectrum as the MAM-2 component from Mamatwan (Fig. 4). Because the Wessels region was universally affected by the Mamatwan-type diagenetic alteration prior to the subsequent Mesoproterozoic, Wessels-type enrichment (Beukes et al., 1995; Gutzmer and Beukes, 1995), we interpret all of our west-northwest downward directions as a consanguineous, postdiagenetic signature carried by the low unblocking temperature, moderate coercivity, neofomed hematite (II).

All but one of the Mn-rich samples from N'chwane II (HMN 6-10) and Wessels (HWS 6-8) also exhibited a shallow, southerly component, removed between 325° and 500°C and constituting a minor portion (5-20%) of the samples' NRM intensities (Fig. 4). Localization of this component (WESS) entirely within the Wessels region, which is strongly affected by Mesoproterozoic hydrothermal alteration (Gutzmer

and Beukes, 1995; Beukes et al., 1995), suggests that WESS is related to that metasomatic episode. In support of that interpretation are the strong ferromagnetic characteristics of these samples similar to those reported by Gutzmer et al. (1995), confined within Wessels-altered ore zones (Fig. 3B). There is no indication of a high unblocking temperature component in these samples; thus coarse-grained (0.1-1.0 mm) neofomed hematite (III), a minor constituent of the Wessels-type ore (Gutzmer and Beukes, 1996), appears not to carry a paleomagnetic remanence or possibly contributes only at unblocking temperatures of <500°C. Again, the petrographically observed grain size of hematite (III), and thus its placement well within the multidomain field (Kletetschka et al., 2000), is consistent with its lack of a high coercivity or high unblocking temperature remanence.

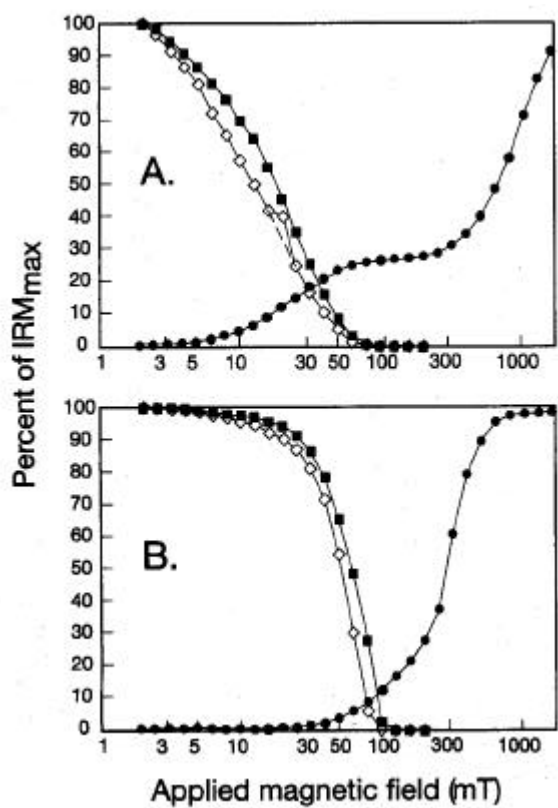


FIG. 3. Rock magnetic properties of representative samples from the Kalahari manganese field. A. HMS 4 = low-grade ore from Mamatwan. Not spurious measurement at 25 mT, omitted by dashed curve segment. B. HML 6 = high-grade Wessels-type hausmannite ore. Solid circles = sequential acquisition of isothermal-remnant magnetization (IRM); open diamonds = sequential alternating-field (AF) demagnetization of IRM; solid squares = sequential AF demagnetization of anhysteretic remanent magnetization (ARM). Both samples exhibit positive modified Lowrie-Fuller tests (Johnson et al., 1975), where coercivity of ARM is higher than that of IRM. This indicates single-domain behavior within the magnetic remanence carriers.

From the N'chwane II and Wessels mines, samples hematitized Mn ore adjacent to the Mesoproterozoic fault zone (HMN 2-5) and jaspilitic iron-formation from the Mn orebody footwall (HWS 2-5), both yielded stable endpoint components that persisted to 675°C (Fig. 5). These directions are highly dispersed, generally streaking between the MAN- direction and the antipode of WESS (Fig. 5D). In addition footwall jaspilites contain a minor component, removed between 400° and 540°C, with a direction similar to WESS but also scattered and perhaps streaked toward the antipode of MAM-2 ( $D = 156.0^\circ$ ,  $I = -32.9^\circ$ ,  $\alpha_{95} = 19.6^\circ$ ; Fig. 5C). In these samples, the remanence-bearing hematite (IV, V, etc.) occupies a very broad range of grain sizes, from ~1  $\mu\text{m}$  to well over 1 mm. The largest grains have a coarse-grained platy habit and clearly formed during the latest stages of Wessels-type alteration. These latest generations of hematite have probably grown from recrystallization of earlier, coarse-grained hematite (III) or, in the case of the altered footwall jaspilites oxidation of sedimentary magnetite to martite (hematite pseudomorph after magnetite). In both cases we might expect a significant inheritance of crystallization remanence from the earlier ferromagnetic phases (Heider and Dunlop

1987) and possibly even self-reversal, consistent with the streaked distribution of observed directions between MAM-2 and WESS. We have not assigned any tectonic significance to these scattered and streaked directions.

Degrees of clustering of the various component directions are statistically indistinguishable when compared before or after tilt correction (Table 2). Therefore, in each case we have decided whether or not to apply tectonic corrections based on the mineral paragenetic relationships described above, in the context of the allowable age range for regional deformation. Open folding of the Kalahari manganese field occurred largely prior to Gamagara-Mapedi red-bed deposition (Beukes and Smit, 1987) at 2060 to 2200 Ma (Beukes et al., 1999) and/or possibly somewhat during the Kheis orogeny at 1750 to 1800 Ma (Stowe, 1983; Cornell et al., 1998). We consider the MAM-1 component in tilt-corrected coordinates, because its microcrystalline hematite (I) carrier, preserved within the early diagenetic microcrystalline matrix, almost certainly formed prior to folding. The MAM-2 remanence acquisition may have occurred either before, during, or after tilting, so it is considered in both pre- and postfold coordinate systems as end-member possibilities. Finally, WESS is demonstrably late Mesoproterozoic in age and its paleomagnetic pole is thus calculated in present coordinates. Note that all tectonic deformation within the Kalahari manganese field is minor (dips less than 20° throughout), so these corrections are all of second order. Although the manganese orebodies have undergone compaction to as little as 60 to 70 percent of their initial thickness during the Wessels alteration event, the process involved removal of layers rather than penetrative pure shear (Gutzmer and Beukes, 1997); therefore, our measured inclinations of premetasomatic magnetic components should remain unbiased.

The tilt-corrected Fisher (1953) mean direction for the early diagenetic MAM-1 component is ( $D = 276.4^\circ$ ,  $I = -10.8^\circ$ ,  $k = 38.2$ ,  $\alpha_{95} = 11.0^\circ$ ). The late diagenetic or early lowgrade metamorphic MAM-2 mean direction is ( $D = 295.2^\circ$ ,  $I = 34.5^\circ$ ,  $k = 59.2$ ,  $\alpha_{95} = 5.2^\circ$ ) in present coordinates or ( $D = 296.4^\circ$ ,  $I = 25.6^\circ$ ,  $k = 45.8$ ,  $\alpha_{95} = 5.9^\circ$ ) in tilt-corrected coordinates. The higher grade, metasomatic WESS component mean direction is ( $D = 186.3^\circ$ ,  $I = -15.7^\circ$ ,  $k = 48.5$ ,  $\alpha_{95} = 8.8^\circ$ ) in present coordinates. Taken as a suite, these directions support what could be called a positive mineralogical (chemical) contact test, akin to the more standard (thermal) baked contact test in paleomagnetism. For example, the equivalent correspondence between WESS and hematitization adjacent to fault zones, coupled with the distinct MAM-1 and MAM-2 direction preserved away from the faults, indicates that the WESS component is the same age as the fault-fed hydrothermal alteration, and that MAM-1 and MAM-2 both antecede the Wessels event. Like a thorough baked contact test, the mineralogical contact test introduced here is bolstered by samples of intermediate composition (HMN 6-10, HWS 6-8), that contain the "country-rock" MAM-2 direction as well as a partial WESS overprint.

#### Discussion

Our paleomagnetic results constrain certain aspects of mineralogical evolution within the Kalahari manganese field. First, Mamatwan-type ore (samples HMS 1-5) contains only

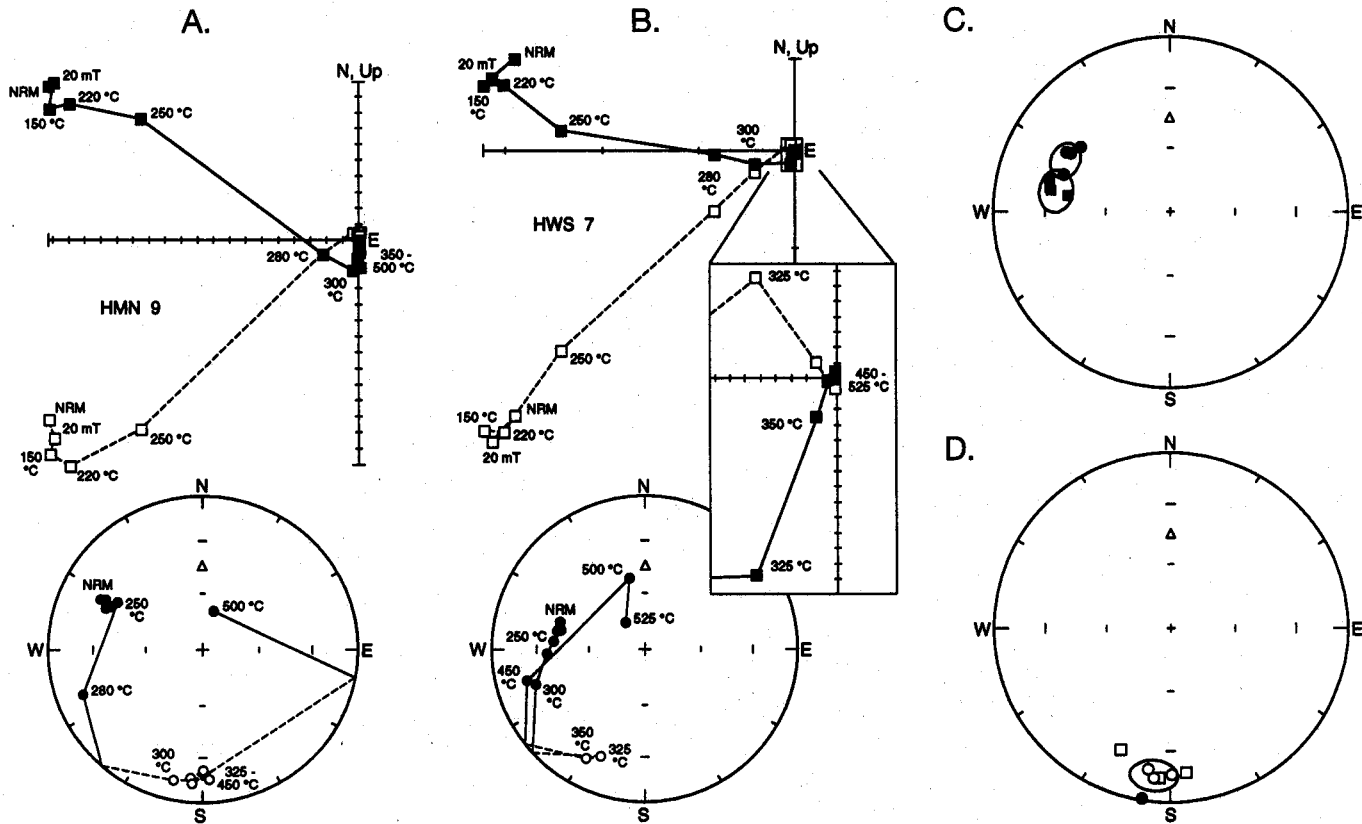


FIG. 4. Paleomagnetic data from Wessels-type hausmannite ore at N'chwaning II (HMN 6-10) and Wessels (HWS 6-8). A. Representative demagnetization behavior, in present coordinates, of specimens HMN 6-10; orthogonal projection tick marks 10-E A/m. B. Representative demagnetization behavior, in present coordinates, of specimens HWS 6-8; orthogonal projection tick marks 1 A/m (inset 10-2 A/m). C. In situ least-squares MAM-2 component directions and their Fisher means (circles = HMN 6-10, squares = HWS 6-8). D. In situ least-squares WESS component directions and their Fisher mean (circles = HMN 6-10, squares = HWS 6-8). Symbols as in Figure 2.

two ferromagnetic minerals of the appropriate compositions and grain sizes for preserving ancient remanence: single-domain hematite, present as a stable endpoint component persisting to 675°C, and medium-grained hematite, removed by 400°C. This agrees well with petrographic observations of the two hematite phases (I, II) as omnipresent constituents of the low-grade, Mamatwan-type ore (Kleyenstüber, 1984; Nel et al., 1986; Gutzmer and Beukes, 1996). Second, the moderate Wessels-type alteration that produced high-grade hausmannite ore (samples HMN 6-10, HWS 6-8) has indeed consumed the diagenetic hematite (I), for we do not observe a stable endpoint magnetic component in these samples. Third, Fe-rich hausmannite (IIa) and hematite (III) that formed during the Wessels event of hydrothermal alteration carry a unique magnetic signature, clearly isolated despite lingering uncertainties regarding its exact mode of origin (Gutzmer et al., 1995; Baron et al., 1998). Finally, multiple episodes of hematitization (IV, V etc.) dominated the apex of Wessels-type alteration in the manganese orebodies, restricted to zones immediately adjacent to the normal faults. This is evidenced clearly by the high-temperature (675°C) stable endpoint components in samples HMN 2-5 and HWS 2-5, despite their high dispersion of remanence directions. All of

these observations are compatible with petrographic observations from the Kalahari manganese field (Gutzmer and Beukes, 1996) and experiment magnetic stability fields for Fe-rich hausmannite (Gutzmer et al., 1995) and hematite (Kletetschka et al., 2000).

When considered in light of previously compiled paleomagnetic results from the Kalahari craton (Evans et al., in press), our results can help discriminate among the various proposed models of ore formation within the Kalahari manganese field. First, a single-stage, exhalative model for manganese enrichment (Cornell and Schutte, 1995) is contradicted by our dataset, which bears three statistically distinct directions of remanence held by the various generations of hematite and hausmannite, acquired as the Kalahari craton shifted latitudes and orientations relative to the geomagnetic dipole reference frame. If the Kalahari manganese field orebody evolution had occurred syngenetically with extrusion of the underlying Ongeluk lavas, then we would expect all of our paleomagnetic directions to be aligned with those from the Ongeluk succession (Evans et al., 1997). In fact, only the MAM-1 direction is similar to the shallow east-west remanence held by the Ongeluk lavas, a fact discussed more thoroughly below. For similar reasons, an entirely metasomatic

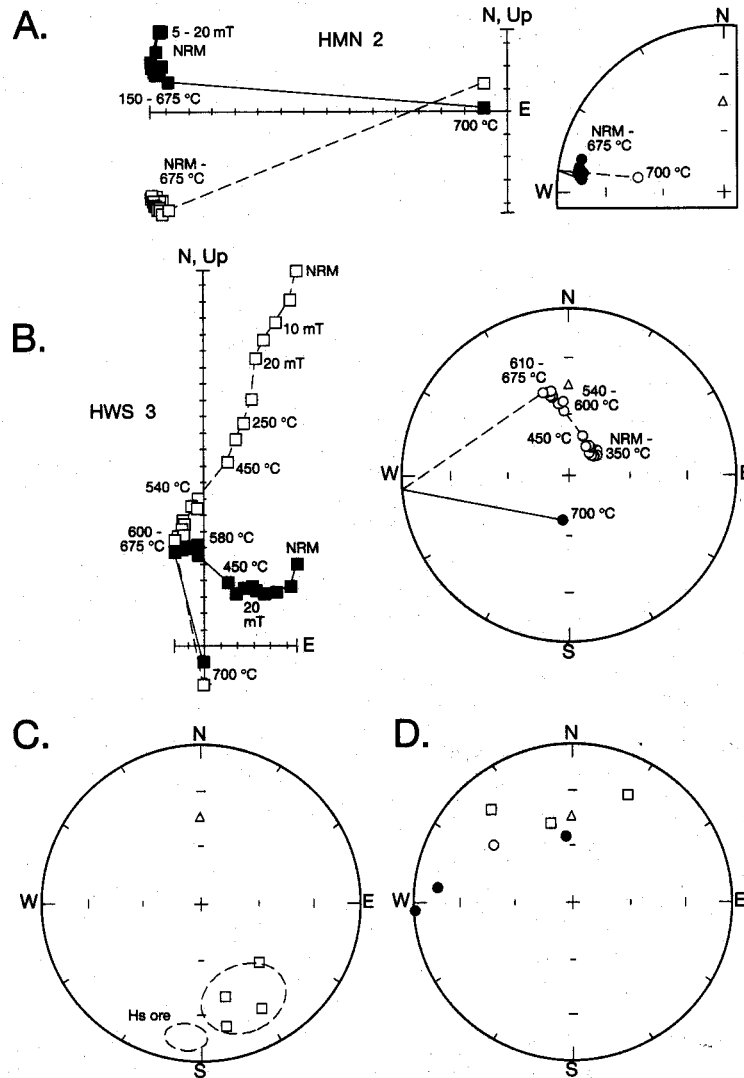


Fig. 5. Paleomagnetic data from hematitized, fault-adjacent zones in the manganese orebody at N'chwaning II (HMN 2-5) and in the footwall jaspilite at Wessels (HWS 2-5). A. Representative demagnetization behavior, in present coordinates, of specimens HMN 2-5; orthogonal projection tick marks 10- A/m. B. Representative demagnetization behavior, in present coordinates, of specimens HWS 2-5; orthogonal projection tick marks 10- A/m. C. In situ least-squares directions from the 400° to 540°C unblocking temperature component of specimens HWS 2-5 and their Fisher mean. The WESS mean uncertainty oval from Figure 4 (Hs ore) is shown for comparison. D. In situ least-squares stable endpoint component directions from both HMN 2-5 (circles) and HWS 2-5 (squares). Symbols as in Figure 2.

origin for all of the various grades of mineralization in the Kalahari manganese field (de Villiers, 1983, 1992) is contradicted by our multidirectional dataset.

Our results support remarkably well the most detailed models-based on independent, petrographic, isotopic, and field evidence-for the timing of ore-forming events in the Kalahari manganese field (Gutzmer and Beukes, 1996). The MAM-1 magnetic remanence, carried by early diagenetic hematite (I) of the Mamatwan-type ore, yields a tilt-corrected paleomagnetic pole at  $(-08.2^{\circ} \text{ N}, 111.1^{\circ} \text{ E})$   $dp = 5.6^{\circ}$ ,  $dm = 11.1^{\circ}$ ). This position corresponds well with that determined from a regional survey of paleomagnetic sites in the immediately underlying Ongeluk lavas (Evans et al., 1997; Fig. 6A). The Kaapvaal craton drifted little between Ongeluk volcanism

and Hotazel Formation diagenesis, supporting the notion of merely a short time interval separating those two events.

Gutzmer and Beukes (1996) postulated that regional metamorphism of the Kalahari manganese field, introducing hematite (II) among other minerals, was related to the 1750 to 1800 Ma Kheis orogeny (Stowe, 1983; Cornell et al., 1998). Our MAM-2 direction corresponds to this regional low-grade metamorphism, regardless of the precise age. Unfortunately, there is no existing paleomagnetic pole for the Kheis event by which to compare our new MAM-2 result. The Kaapvaal craton has a well-established mid-Paleoproterozoic apparent polar wander path beginning with poles from the 2060 Ma Phalaborwa and Bushveld Complexes and extending westward toward poles from the 1800 to 1900 Ma Mashonaland

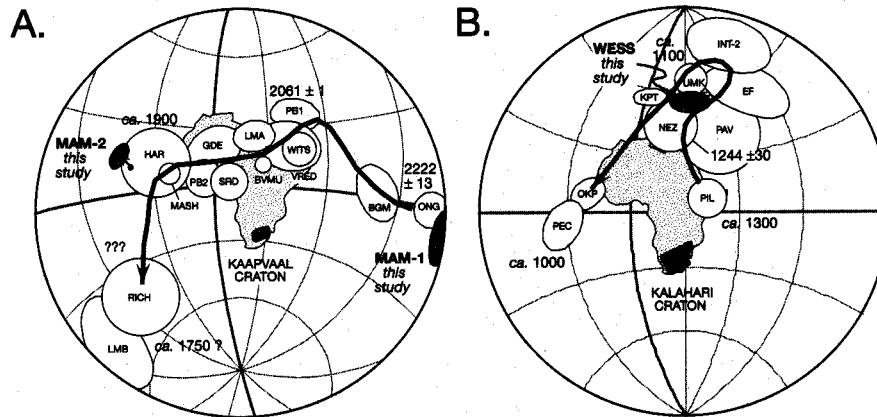


Fig. 6. Comparison of paleomagnetic poles from the Kalahari manganese field (this study) with previous results from the Kaapvaal-Kalahari craton. For descriptions of paleomagnetic poles and references see Evans et al. (in press). A. Paleoproterozoic; equal-angle projection centered on  $15^{\circ}$  S,  $015^{\circ}$  E. Arrow of MAM-2 denotes the effect of tilt correction. BGM = basal Gamagara-Mapedi; BVMU = Bushveld Main and Upper zones; GDE = Great Dyke extensions; HAR = Hartley lava; LMA, LMB = Limpopo "A" and "B" components; MASH = Mashonaland sills; ONG = Ongeluk lava; PB1, PB2 = Phalaborwa "1" and "2" components; RICH = Richtersveld; SRD = Sand River dikes; VRED = Vredefort impact; WITS = Witwatersrand overprint. B. Mesoproterozoic; equal-angle projection centered on  $00^{\circ}$  N,  $030^{\circ}$  E. Ages in Ma. EF = Ezelfontein Formation; INT-2 = intermediate component "2" from Sishen iron ore; KPT = Kalkpunt Formation; NEZ = Namaqua eastern zone; OKP = Okiep intrusions; PEC = Port Edward Charnockite; PIL = Pilanesberg dikes; PAV = Premier kimberlite field average pole; UMK = Umkondo igneous suite.

dolerites in Zimbabwe (undoubtedly connected to Kaapvaal by that time) and the ca. 1900 Ma Hartley lavas of the Olifantshoek Supergroup that unconformably overlies the Ongeluk-Hotazel succession in Griqualand West (reviewed by Evans et al., in press; Fig. 6A). The Mashonaland and Hartley igneous units are broadly coeval-possibly consanguineous with the poorly dated Sibasa basalt (Soutpansberg Group) and Sand River dikes (Barton and Pretorius, 1997) and related to the ca. 1900 Ma rift stage of a Wilson cycle (Cornell et al., 1998). Our MAM-2 pole lies just beyond the Mashonaland and Hartley results along the apparent polar wander path (Fig. 6A; Evans et al., in press) and so may result from extension-related magmatism that expelled stratabound fluids into the Kalahari manganese field. Alternatively, MAM-2 could be due to foreland-driven orogenic fluids from the Kheis fold thrust episode (Gutzmer and Beukes, 1996), loosely dated at 1700 to 1800 Ma (Stowe, 1983; Cornell et al., 1998). Both the rift- and Kheis-related tectonic models for MAM-2 would be consistent with the various crosscutting relationships observed in the Kalahari manganese field (Gutzmer and Beukes, 1996).

Existing regional crosscutting relationships and isotopic data from the Kalahari manganese field suggested a late Mesoproterozoic age for the Wessels event (Dixon, 1989), thereby associating it with tectonothermal activity in the Namaqua orogen (Gutzmer and Beukes, 1996). Our WESS paleomagnetic pole may help refine the age of Wessels hydrothermal alteration, through comparisons with previously determined, well-dated paleomagnetic poles from the Kalahari craton. Evans et al. (in press), following Onstott et al. (1986), summarized the existing database and determined a large loop of paleomagnetic poles that sweeps twice through northernmost Africa, at ca. 1240 and 1100 Ma (Fig. 6B). Our WESS paleomagnetic pole lies at the knot of this apparent polar wander loop, adjacent to paleomagnetic poles from the

Namaqua eastern zone (NEZ;  $1244 \pm 30$  Ma; Onstott et al., 1986; Evans et al., in press) the Premier kimberlite field (PAV, ca. 1200 Ma; Doppelhammer and Hargraves, 1994), and the Umkondo igneous event (UMK,  $1105 \pm 2$  Ma; Hargraves et al., 1994; Hanson et al., 1998). Other poles that are nearby but significantly distinct are from the ca. 1170 Ma Koras Group (Gutzmer et al., 2000) volcanics and red beds (EF and KPT, Ezelfontein and Kalkpunt-Florida Formations; Briden et al., 1979). The well dated, ca. 1000 Ma poles from the Okiep Norite and Port Edward Charnockite (OKP and PEC; Onstott et al., 1986) are greatly separated from the 1250/1100 Ma apparent polar wander loop. The Pilanesberg dikes yield a paleomagnetic pole (PIL; Gough, 1956) with an age of ca. 1300 Ma (Van Niekerk, 1962), also widely separated from our WESS result. It may be surmised, then, that ages of ca. 1250 and 1100 Ma for the Wessels hydrothermal event are consistent with the present paleomagnetic database, but that younger ages of ca. 1000 Ma are not. An older age of ca. 1300 Ma for the Wessels alteration, as reported by Dixon (1989), can only be compatible with the paleomagnetic data if the Pilanesberg dikes are in fact significantly older than 1300 Ma (perhaps still within the uncertainty of the mean age).

Wessels-type alteration, occurring in the foreland of the late Mesoproterozoic Namaqua orogen, can thus be linked temporally to the early stages of tectonic activity within that fold belt. Our data support the earlier inference (Gutzmer and Beukes, 1996) of a genetic relationship between the Namaqua orogeny and Wessels-related hydrothermal metasomatism. The paleomagnetically permissible ages of ca. 1250 or 1100 Ma for such an episode correlate well with the isotopic evidence for substantial diachroneity of the Namaqua belt, ca. 1000 Ma deformation being restricted largely to the western sectors of the orogen (Botha et al., 1979; Onstott et al., 1986). Finally, these results provide further evidence that Namaqua-related deformation or tectonothermal activity

transgressed eastward across the Kheis province and onto the Kaapvaal craton (Moen, 1999; Evans et al., in press).

#### Acknowledgments

We thank the geologic staff of Assmang Ltd. at Black Rock and Samancor Ltd. at Hotazel for logistical support. Reviews by Rob Hargraves and Pierre Hattingh led to an improved manuscript. This project is also funded by grants from the United States National Science Foundation (EAR94-18523) and National Research Foundation (Pretoria). D.A.D.E. is supported by an Australian Research Council postdoctoral fellowship: Tectonics Special Research Centre contribution 127.

June 26, December 4, 2000

#### REFERENCES

- Abs Wurbach, I., Hewat, A.W., and Sabine, T.M., 1981, Magnetische- und Neutronenbeugungs-Experimente an Braunit,  $Mn^{2+}Mn^{3+}_2O_8/SiO_4$ : Zeitschrift für Kristallographie, v. 154, p. 240-242.
- Baron, V., Gutzmer, J., Rundlof, H., and Tellgren, R., 1998, The influence of iron substitution on the magnetic properties of hausmannite  $Mn^{2+}(Fe, Mn)^{3+}_2O_4$ : American Mineralogist, v. 83, p. 786-793. [See also erratum: v. 84, p. 212]
- Barton, J.M., Jr., and Pretorius, W., 1997, The lower unconformity-bounded sequence of the Soutpansberg Group and its correlatives—remnants of a Proterozoic large igneous province: South African Journal of Geology, v. 100, p. 335-339.
- Bau, M., Romer, R.L., Lüders, V., and Beukes, N.J., 1999, Pb, O, and C isotopes in -silicified Mooidraai dolomite (Transvaal Supergroup, South Africa): Implications for the composition of Paleoproterozoic seawater and "dating" the increase of oxygen in the Precambrian atmosphere: Earth and Planetary Science Letters, v. 174, p. 43-57.
- Beukes, N.J., 1983, Palaeoenvironmental setting of iron formations in the depositional basin of the Transvaal Supergroup, South Africa, to Trendall, A.F., and Morris, B.C., eds., Iron formations: Facts and problems: Amsterdam, Elsevier, p. 131-209.
- Beukes, N.J., and Gutzmer, J., 1996, A volcanic-exhalative origin for the world's largest (Kalahari) manganese field: A discussion of the paper by D.H. Cornell and S.S. Schütte: Mineralium Deposita, v. 31, p. 242-245.
- Beukes, N.J., and Smit, C.A., 1987, New evidence for thrust faulting in Griqualand West, South Africa: Implications for stratigraphy and the age of red beds: South African Journal of Geology, v. 90, p. 378-394.
- Beukes, N.J., Burger, A.M., and Gutzmer, J., 1995, Fault-controlled hydrothermal alteration of Palaeoproterozoic manganese ore in Wessels mine, Kalahari manganese field: South African Journal of Geology, v. 98, p. 430-451.
- Beukes, N.J., Gutzmer, J., and Dorland, H., 1999, Palaeoproterozoic laterites, supergene iron and manganese ores and atmospheric oxygen [abs]: Geological Society of Australia Abstracts, no. 56, p. 7A-7D.
- Botha, B.J.V., Grobler, N.J., and Burger, A.J., 1979, New U-Pb age-measurements on the Koras Group, Cape Province and its significance as a time-reference horizon in eastern Namaqualand: Geological Society of South Africa Transactions, v. 82, p. 1-10.
- Briden, J.C., Duff, B.A., and Kroner, A., 1979, Palaeomagnetism of the Koras Group, northern Cape Province, South Africa: Precambrian Research, v. 10, p. 43-57.
- Cairncross, B., Beukes, N.J., and Gutzmer, J., 1997, The manganese adventure: The South African manganese fields: Johannesburg, Associated Ore and Metal Corporation, 236 p.
- Cornell, D.H., and Schütte, S.S., 1995, A volcanic-exhalative origin for the world's largest (Kalahari) manganese field: Mineralium Deposita, v. 30, p. 146-151.
- Cornell, D.H., Schütte, S.S., and Eglington, B.L., 1996, The Ongeluk basaltic andesite formation in Griqualand West, South Africa: Submarine alteration in a 2222 Ma Proterozoic sea: Precambrian Research, v. 79, p. 101-123.
- Cornell, D.H., Armstrong, R.A., and Walraven, F., 1998, Geochronology of the Proterozoic Hartley Formation, South Africa: Constraints on the Kheis tectogenesis and the Kaapvaal craton's earliest Wilson cycle: Journal of African Earth Sciences, v. 26, p. 5-27.
- de Villiers, J.E., 1983, The manganese deposits of Griqualand West, South Africa: Some mineralogical aspects: Economic GEOLOGY, v. 78, p. 1108-1118.
- 1992, On the origin of the Griqualand West manganese and iron deposits: South African Journal of Science, v. 88, p. 12-15.
- Dixon, R.D., 1989, Sugilite and associated metamorphic silicate minerals from Wessels mine, Kalahari manganese field: South African Geological Survey Bulletin 93, 47 p.
- Doppelhammer, S.K., and Hargraves, R.B., 1994, Paleomagnetism of the Schuller and Franspoort kimberlite pipes in South Africa and an improved Premier pole: Precambrian Research, v. 69, p. 193-197.
- Dunlop, D.J., and Ozdemir, T., 1997, Rock magnetism: Fundamentals and frontiers: Cambridge, Cambridge University Press, 573 p.
- Evans, D.A.D., Beukes, N.J., and Kirschvink, J.L., 1997, Low-latitude glaciation in the Palaeoproterozoic era: Nature, v. 386, p. 262-266.
- 2000, Paleomagnetism of a lateritic paleo-weathering horizon and overlying Paleoproterozoic redbeds from South Africa: Implications for the Kaapvaal apparent polar wander path and a confirmation of atmospheric oxygen enrichment: Journal of Geophysical Research, in press.
- Fisher, R.A., 1953, Dispersion on a sphere: Royal Society of London Proceedings v. A217, p. 295-305.
- Gough, D.I., 1956, A study of the palaeomagnetism of the Pilansberg dykes: Royal Astronomical Society Monthly Notices, Geophysical Supplement, v. 7, p. 196-213.
- Grant, R.W., Geller, S., Cape, J.A., and Espinosa, G.P., 1968, Magnetic and crystallographic transitions in the a-MnO<sub>3</sub>-FeO<sub>3</sub> system: Physical Review, v. 175, p. 686-695.
- Gutzmer, J., and Beukes, N.J., 1995, Fault controlled metasomatic alteration of Early Proterozoic sedimentary manganese ores in the Kalahari manganese field, South Africa: Economic GEOLOGY, v. 90, p. 823-844.
- 1996, Mineral paragenesis of the Kalahari manganese field, South Africa: Ore Geology Reviews, v. 11, p. 405-428.
- 1997, Effects of mass transfer, compaction and secondary porosity on hydrothermal upgrading of Paleoproterozoic sedimentary manganese ore in the Kalahari manganese field, South Africa: Mineralium Deposita, v. 32, p. 250-256.
- Gutzmer, J., Beukes, N.J., Kleyenstüber, A.S.E.; and Burger, A.M., 1995, Magnetic hausmannite from hydrothermally altered manganese ore in the Palaeoproterozoic Kalahari manganese deposit, Transvaal Supergroup, South Africa: Mineralogical Magazine, v. 59, p. 703-716.
- Gutzmer, J., Beukes, N.J., Pickard, A., and Barley, M.E., 2000, 1170 Ma SHRIMP age for Koras Group bimodal volcanism, northern Cape Province: South African Journal of Geology, v. 103, p. 32-37.
- Hanson, R.E., Martin, M.W., Bowring, S.A., and Munyanyiwa, H., 1998, U-Mn zircon age for the Umkondo Dolerites, eastern Zimbabwe; 1.1 Ga large igneous province in southern Africa-East Antarctica and possible Rodinia connections: Geology, v. 26, p. 1143-1146.
- Hargraves, R.B., Hattingh, P.J., and Onstott, T.C., 1994, Palaeomagnetic results from the Timbavati gabbros in the Kruger National Park, South Africa: South African Journal of Geology, v. 97, p. 114-118.
- Heider, F., and Dunlop, D.J., 1987, Two types of chemical remanent magnetization during oxidation of magnetite: Physics of the Earth and Planetary Interiors, v. 46, p. 24-45.
- Johnson, H.P., Lowrie, W., and Kent, D.V., 1975, Stability of ARM in fine and coarse magnetite and maghemite particles: Royal Astronomical Society Geophysical journal, v. 41, p. 1-10.
- Kirschvink, J.L., 1980, The least-squares line and plane and the analysis of palaeomagnetic data: Royal Astronomical Society Geophysical journal, v. 62, p. 699-718.
- Kirschvink, J.L., Gaidos, E.J., Bertani, L.E., Beukes, N.J., Gutzmer, J., Maepa, L.N., and Steinberger, R.E., 2000, Paleoproterozoic Snowball Earth: Extreme climatic and geochemical global change and its biological consequences: National Academy of Sciences Proceedings, v. 97, p. 1400-1405.
- Kletetschka, G., Wasilewski, P.J., and Taylor, P.T., 2000, Unique thermoremanent magnetization of multidomain sized hematite: Implications for magnetic anomalies: Earth and Planetary Science Letters, v. 176, p. 469-479.
- Kleyenstüber, A.S.E., 1984, *The mineralogy of the manganese-bearing Hotazel Formation; of the Proterozoic Transvaal sequence in Griqualand West, South Africa: Geological Society of South Africa Transactions, v. 87, p. 257-272.*
- Lüders, V., Gutzmer, J., and Beukes, N.J., 1999, Fluid inclusion studies in co-genetic hematite, hausmannite, and gangue minerals from high-grade

- Moen, H.F.G., 1999, The Kheis tectonic subprovince, southern Africa: A lithostratigraphic perspective: *South African Journal of Geology*, v. 102, p. 27-42.
- Nel, C.J., Beukes, N.J., and de Villiers, J.P.R., 1986, The Mamatwan manganese mine of the Kalahari manganese field, in Annhaeusser, C. R., and Maske, S., eds., *Mineral deposits of southern Africa*: Johannesburg, Geological Society of South Africa, v. 1, p. 963-978.
- Onstott, T.C., Hargraves, R.B., and Joubert, P., 1986, Constraints on the tectonic evolution of the Namaqua province II: Reconnaissance palaeomagnetic and  $^{40}\text{Ar}/^{39}\text{Ar}$  results from the Namaqua province and Kheis belt: *Geological Society of South Africa Transactions*, v. 89, p. 143-170.
- Pullaiah, G., Irving, E., Buchan, K.L., and Dunlop, D.J., 1975, Magnetization changes caused by burial and uplift: *Earth and Planetary Science Letters*, v. 27, p. 147-171.
- Stowe, C.W., 1983, The Uppington geotraverse and its implications for craton margin tectonics: *Geological Society of South Africa Special Publication*, v. 10, p. 147-171.
- Taneja, S.P., and Garg, V K., 1993, Mossbauer and magnetic study of braunite mineral: *Nuclear Instruments and Methods in Physics Research B*, v. 76, p. 239-241.
- Tsikos, H., and Moore, J.M., 1998, The Kalahari manganese field: An enigmatic association of iron and manganese: *South African Journal of Geology*, v. 101, p. 287-290.
- Van der Voo, R., 1990, The reliability of paleomagnetic data: *Tectonophysics*, v. 184, p. 1-9.
- Van Niekerk, C.B., 1962, The age of the Gemspost dyke from the Venterspost gold mine: *Geological Society of South Africa Transactions*, v. 65, p. 105-111.